IRON SULFIDE DEPOSITION DURING COAL GASIFICATION

D. Duane Brooker and Myongsook S. Oh,
Texaco R&D, P.O. Box 509, Beacon, NY 12533

Keywords: Gasification, ash, iron sulfide

INTRODUCTION

The partial combustion of coal under reducing conditions in entrained gasifiers and fluidized beds is becoming more prevalent. However, very little information on ash deposition chemistry from operating units has been published. Instead, most of the work that has been done is based on thermodynamic calculations, or laboratory experimentation associated with these calculations[1,2,3]. The thermodynamic calculations often indicated that calcium or sodium sulfide can form as a sticky slag phase at low temperatures, while iron sulfide should be the prevalent at higher temperatures.

Analyses of deposits from the Cool Water Coal Gasification Project did not identify any calcium, sodium, nor solid solution of sodium-calcium-iron sulfides in the SUFCo ash[4]. Iron sulfide was observed around most fly ash particles, but it could not be determined if the sulfide was formed from vapor deposition, reaction of H_2S from the gas with iron in the flyash, or wetted the surface of the siliceous spheres during gasification. Layers of iron sulfide that had encapsulated flyash particles within it were noted on water wall tubing and within the deposit. Based on these layers, vapor or fume deposition of iron sulfide was thought to have occurred. However, at normal gasification temperatures (1300-1500°C), iron sulfide is expected to occur as a liquid phase, not in the vapor state.

An additional opportunity to study iron sulfide deposit formation during gasification occurred during a hot gas clean-up run at Texaco's Montebello Research Laboratory. Pitts. #8, a high iron bituminous coal, was gasified during this test. Analysis of the samples yielded similar results as with the SUFCo ash from Cool Water, in that iron and sulfur were enriched on the outer surface of the siliceous flyash particles. However, unlike the Cool Water deposit analyses where distinct iron sulfide crystals were not observed, numerous euhedral iron sulfide crystals, some with siliceous spheres encapsulated in them, formed in the Pitts. #8 deposit. Again, no sodium or calcium sulfides were observed. In order to gain a better understanding of deposit formation mechanisms during gasification, detailed analyses of the Pitts. #8 deposits were done.

PROCESS DESCRIPTION

The Texaco coal gasification process involves the partial combustion of a water-coal slurry with oxygen in a refractory lined vessel[5]. Operating pressure in the unit ranges from 21-63 atm. while the operating temperatures varies from 1260-1538°C. The typical partial pressure of oxygen is approximately 10^{-11} atm. while the partial pressure of sulfur is 10^{-5} atm. at gasification temperatures. Carbon conversion is over 99%. During gasification, the inorganic material encapsulated in the coal particles forms small, molten, spherical (submicron to 100 micron) particles that either impact on the refractory lined wall to form a molten slag layer, or is entrained in the synthesis gas (syngas) exiting the vessel. Depending on the end use of the

syngas, the gas can be cooled by direct water quench, or partially cooled by passing it through a syngas cooler. Once through the cooler, the syngas is then scrubbed and cooled to remove over 99% of the sulfur. In an alternate mode of gas clean-up (hot gas clean-up), the particualte can be removed by ceramic cross-flow filters, and the sulfur captured by inorganic sorbents. Ultimately, the syngas is fed to a gas turbine for electric production, or used as process gas for chemical production.

Following a 20 hour test run for hot gas clean-up using Pitts. #8 coal, deposits were removed from a bend in a refractory lined gas transfer line exiting from a radiant syngas cooler at Texaco's pilot unit in Montebello, CA. Gasification temperatures during this run were between 1370-1482°C. The thermocouple in the transfer line indicated that the gas temperature was between 870-932°C in the area of deposition. No additives or slag modifiers were used with the coal. The initial ash chemistry of Pitts. #8 is given in Table I.

SAMPLE ANALYSIS

The deposit was removed from the transfer line without exposing them to water. Pieces of castable refractory were adhered to the outer surface of the deposit. The deposit was dark grey in color and friable in most areas. Layering occurred throughout the deposit and consisted of glass-like materials intermixed with less dense, sintered ash. Stringers of harder ash formed throughout the less sintered ash. Polished sections were made using standard reflective light polishing procedures for microscopic analyses.

A JEOL 6300 scanning electron microscope (SEM) with an attached Noran Explorer energy dispersive x-ray spectrometer (EDS) was used to analyze the samples. Chemical analyses were done using a standardless PROZA correction routine. The SEM showed that the hard, dense layers and stringers consisted of devitrofying ash particles, mostly under 2 microns in size. The rate of devitrofication appears to have been controlled mainly by the size of the particles in the layers; e.g. the smaller the particle size, the denser the layer. EDS analysis indicated that the highly sintered layer consisted of calcium alumina silicate and a sintering phase of iron-magnesium alumina silicate. Iron sulfide particles having a similar size as the remnant ash particles occurred throughout this material (Fig. 1). Also found within the highly sintered layer were layers of iron sulfide which contoured the ash layering (Fig. 2). No depletion in iron sulfide or iron were noted around the sulfide layers. However, the overall sulfur in the highly sintered material was lower than the poorly sintered samples.

In the more porous, sintered layers, the particle size increased: many flyash particles were between 5-10 microns in diameter. Deformation was common with many particles, suggesting that the particles were semi-molten at the time of impact. All of these particles were surrounded by iron sulfide droplets and crystals (Fig. 3). Most of these particles consisted of calcium-potassium alumina siliceous glass with magnesium-iron alumina silicates crystallizing within them and on the outer surface.

On the ID (gas side) of the deposit, there was a layer of poorly sinter ash which was the last material to be deposited. In this layer, the flyash particles still maintained their original roundness and showed no signs of recrystallization (Fig. 4). Iron sulfide particles were found on the outside of some of the flyash, but were smaller in size than those in the sintered material.

The deposit chemical composition (Table II) was compared to the clarifier bottom particles (flyash that passed through the transfer line and was water scrubbed from the gas) and slag particles. As seen by the bulk composition, iron is similar in concentration in the slag, clarifier bottoms, and deposit, but the sulfur concentration increases respectively. However, chemical analyses of the individual flyash particles indicate significant differences between those in the clarifier bottom and deposit. The siliceous flyash particles in the deposit are iron poor, potassium and calcium rich compared to the flyash in the clarifier bottoms. In turn the clarifier ash is slightly lower in iron content than the slag. Also, less than 5 % of the clarifier bottom particles are surrounded by iron sulfide.

SEM analysis of broken surfaces of the deposit revealed euhedral iron sulfide crystals up to 1.5 microns on the outside of the larger particles. Some of these particles were growing around the siliceous ash particles into well developed crystals (Fig. 5). X-ray diffraction (done on a Scintag Pad V instrument with a quartz standard) indicated that the sulfide occurred as both troilite and pyrrhotite.

DISCUSSION

Based on the Cool Water and MRL deposits, iron sulfide is the lowest melting phase that occurs in abundant on the outside of the ash particles, and is the most likely bonding phase for the ash. However, the mode-of-formation of the iron sulfide is not as clear based on these analyses. For instance, iron sulfide visibly occurs on the outer surface of less than 5 % of the clarifier flyash while every particle in the deposit is coated by iron and sulfur. The discreet iron sulfide particles found in the clarifier material consist of spheres or fragments mixed with siliceous glass, not euhedral crystals. Also, there exist a clear difference in the clarifier flyash chemical composition which is closer to the composition of the slag, and is much different chemical composition than the ash in the deposit. Based on the analytical evidence from the deposits, the three most likely means of formation of iron sulfide are given below:

1) **Formation of FeS during gasification.** During gasification some of the pyrite in the coal is converted to FeS droplets with small amounts of FeO (iron oxy-sulfides) and Fe within them, and fume particles. The oxy-sulfide droplets migrated to the outer surface of the siliceous ash. Only those ash particles with sufficient iron sulfide on their outer surfaces are sticky enough to be deposited. The thermodynamic calculations indicate that iron oxy-sulfide particles are sticky at deposition site temperature[6]. After deposition, the high temperatures in the transfer line caused crystallization of the glass, and recrystallization of the FeS.

A possible explanation for the difference in chemical composition between the siliceous ash in the clarifier and in the deposit is the associated mineralogy with the pyrite-rich areas in the coal seam (e.g. clay rich praticles were more prevalent). Difficulties with this theory include the formation of the discreet FeS layers within the deposit, and the large size of some of the FeS crystals compared to the loosely bonded ash. Also, not explained is the change in composition among the loosely bonded ash, clarifier bottoms, and ash in the deposit.

2) **Formation of FeS from Vapor Phase Species during Cooling.** After the particles leave the gasifier, a volatile iron species is condensed on the surface of the ash particle and reacts with H_2S upon cooling to produce an FeS coating. A thin layer of iron and sulfur was observed on the outside of the flyash from Cool Water could be indicative of vapor condensation. Other

evidence suggestive of vapor formation include the euhedral nature of the FeS crystal, encapsulation of siliceous particles within these crystals, and the occurrence of discreet FeS layers.

Vapor deposition of FeS from the gas phase does not appear very likely due to the low vapor pressure of FeS. Iron pentacarbonyl, which is a very volatile iron species, is not stable at high temperatures and is not expected to play a role in FeS formation. According to our thermodynamic equilibrium calculations shown in Table III, the only likely species of iron to be volatile is iron chloride, which may combine with the H_2S to form FeS upon cooling. However, the importance of $FeCl_2$ on FeS formation is not very conclusive as indicated by the equilibrium vapor pressure which does not change from 1200 to 900°C

3) **Formation of FeS from Iron in the Glass during Cooling**. During cooling the H_2S in the syngas interacts with iron in the ash. If this mechanism occurs, then iron depletion within the siliceous ash particle should be observed. The identification of iron magnesium alumina silicates on the surface of the ash in the deposit does indicate that iron is being expelled from the glass structure which is recrystallizing to form anorthite. However, no iron depletion was noted around the FeS layers.

Laboratory support of H_2S combining with iron to form euhedral crystals was gained from several experiments conducted by flowing a H_2S-CO-CO_2 gas mixture through a bed of clarifier bottoms ash within a quartz tube. Analysis of the clarifier bottom ash indicated the sulfur content went from 3.3 wt. % to 11.3 wt.%. Within the ash, euhedral cyrstals of iron sulfide were prevalent and of the same size as the deposit.

Quite likely, both mechanisms 1 and 3 are occurring based on the evidence from Pitts. #8 and SUFCo deposits. Hence, the following depositional pathways are believed to have occurred:

1. During gasification iron oxy-sulfide particles and fumes are produced along with siliceous particles containing iron sulfide. The iron sulfide within the siliceous particles migrate to the outer surface of the ash. In the case of Pitts. #8, the FeS_2 particles in the coal may be associated with calcium-potassium alumina silicate clay mineral.

2. The ash particles begin cooling downstream of the reaction chamber, where the gas temperature is still above the solidification point of the FeS and at the softening point of the ash. Additional fume particles collect on the ash. FeS also forms on the outside of the particles due to H_2S combining with the iron within the siliceous glass.

3. FeS fume particles collected on the cooler surface of the gasifier due to thermopheresic effect, thus forming a fouling layer. The ash particles that have the thickest FeS layer around them adhere to the wall in areas of high turbidity. Once adhered to the wall, the glass, which is low melting, begins to sinter and devitrofying forming anorthite and an iron-magnesium alumina silicate.

4. During sintering, the oxy-sulfide particles on the outside of the siliceous particles migrate to pores in the deposit. At temperatures above 1000°C, the iron sulfide already deposited, will recrystallized and combine with additional FeS generated from H_2S reacting with iron from the silicates to form large euhedral crystals of FeS.

CONCLUSIONS

Iron sulfide has been identified as the most likely bonding phase on the outside of flyash particles in both low and high iron coals during partial oxidation within Texaco's gasifers. SEM-EDS analysis has indicated no other elements (e.g. sodium or potassium) were present in the iron sulfide to form a low melting eutectic. Laboratory testing also suggest that the iron sulfide can be generated from H_2S in the gas reacting with iron from the glass in the flyash. The occurrence of discreet layers of iron sulfide within the deposit still remains problematic. Our own research will continue to concentrate on determining the interaction between iron and hydrogen sulfide in partial oxidation systems, by sintering the clarifier bottoms and ash deposits under simulated gasifier conditions.

REFERENCES

1. John, R. C., "Slag, Gas, and Deposit Thermochemistry in a Coal Gasifier", J. Electochemsitry, 133, (1), p205-211

2. Benson, S. A., et. al., "Coal Ash Behavior in Reducing Environment", NDEERC Report, 1992

3. Najjar, M. S. and Jung, D. Y., ACS, Div. of Fuel Chemistry Preprint 35(3), 615, 1990.

4. Brooker, D. D., "Chemistry of Deposit Formation in a Coal Gasifier Syngas Cooler", Fuel, 72(5), 665, 1993.

5. Cool Water Coal Gasification Program: Final Report, EPRI GS-6806, 1990.

6. Levin, E. M. et. al, Phase Diagrams for Ceramist, 1. p522, 1964.

TABLE I
Chemical Composition of Pitts. #8 Coal

	wt.%
Na2O	1.19
MgO	0.48
Al2O3	20.25
SiO2	38.60
P2O5	0.82
K2O	1.56
CaO	4.54
TiO2	1.05
Fe2O3	22.44
SO3	8.40

TABLE II
Chemical Composition In Deposit (SEM-EDS, elemental wt. %)

	Na	Mg	Al	Si	P	S	K	Ca	Fe
BULK									
Gas Side	1.4	2.4	17.7	34.1	0.4	10.9	3.1	8.3	20.1
Interior	1.5	2.0	17.2	31.0	0.7	11.0	2.4	8.7	24.6
Clarifier	2.5	2.1	18.6	31.2	x	3.2	2.8	7.9	27.9
Slag	2.1	1.8	20.6	35.8	x	2.3	2.1	6.0	29.7
Ave. 15 Particles									
Part. Gas Side	1.6	1.7	19.8	41.0	1.0	4.3	2.8	7.0	19.7
Part. Dep	1.5	1.5	19.6	48.1	0.7	1.8	5.0	13.0	7.4
Part. Clar.	1.8	2.2	22.4	40.5	0.3	1.1	3.1	7.2	21.6

Table III. Equilibrium Calculation of Cl and Fe system under TGP conditions.

Possible species and phases in system

GAS		LIQUID
CO (G)	Cl (g)	Fe O (l)
N2 (G)	Cl2 (g)	Fe (l)
H2 (G)	HCl (g)	Fe S (l)
H2 O (G)	Fe (g)	S (l)*
O2 (G)	FeS (g)	
H2 S (G)	FeO (g)	SINGLE
S2 (g)	Fe(CO)5 (g)	Fe (s)
	FeCl2 (g)	FeO (s)
		FeS (s)

Initial input of species

	mole	mole frac
CO (G)	30	0.30
N2 (G)	12.51	0.12
H2 (G)	23.63	0.24
H2 O (G)	33.09	0.33
H2 S (G)	0.75	0.0075
Cl2 (g)	0.014	0.00014
Fe (g)	0.243	0.0024242
System Totals	100.24	

*Temperature limits extended: max 1226.85 to 1300 °C using equation

EQUILIBRIUM STATE OF SYSTEM AT 40.0 ATM

Temp (°C)	1300	1200	1100	1000	900	800	700	600
GAS (Fugacity, atm)								
N_2 (G)	5.01	5.01	5.01	5.01	5.02	5.03	5.03	5.03
CO_2 (G)	12.01	12.01	12.02	12.02	12.03	12.06	12.06	12.06
H_2 (G)	9.45	9.45	9.45	9.45	9.45	9.45	9.45	9.45
H_2 O (G)	13.24	13.24	13.24	13.24	13.24	13.24	13.24	13.24
O_2 (G)	4.5e-11	3.4e-12	1.7e-13	5.5e-15	1.0e-16	8.7e-19	2.9e-21	2.6e-24
H S (G)	0.28	0.27	0.27	0.26	0.26	0.20	0.20	0.20
S_2 (g)	1.2e-04	4.8e-05	1.6e-05	4.3e-06	9.6e-07	1.1e-07	1.3e-08	1.1e-09
Cl (g)	1.2e-07	3.8e-08	1.0e-08	2.2e-09	3.8e-10	4.7e-11	3.8e-12	1.7e-13
Cl_2 (g)	1.6e-12	6.1e-13	2.0e-13	5.4e-14	1.2e-14	1.9e-15	2.2e-16	1.5e-17
Cl H (G)	1.1e-02	1.1e-02	1.1e-02	1.1e-02	1.1e-02	1.1e-02	1.1e-02	1.1e-02
Fe (g)	1.3e-07	1.7e-08	1.5e-09	9.1e-11	3.2e-12	5.1e-14	2.1e-16	2.4e-19
FeS (g)	4.0e-08	5.5e-09	5.6e-10	3.8e-11	1.5e-12	2.3e-14	1.2e-16	1.9e-19
FeO (g)	1.0e-09	8.4e-11	4.7e-12	1.6e-13	3.0e-15	2.2e-17	3.6e-20	1.4e-23
$Fe(CO)_5$ (g)	1.9e-19	4.0e-19	9.5e-19	2.6e-18	8.2e-18	2.9e-17	8.2e-17	3.1e-16
$FeCl_2$ (G)	2.4e-06	2.0e-06	1.6e-06	1.2e-06	7.8e-07	4.1e-07	1.2e-07	2.5e-08
LIQUID (gram)								
Fe O (l)	10.37	9.935	9.389	8.704	7.85	0	0	0
Fe (l)	2.371	2.189	1.974	1.723	1.438	0	0	0
Fe S (l)	4.938	5.759	6.767	7.999	9.493	0	0	0
S (l)	0.0045	0.0035	0.0026	0.0019	0.0013	0	0	0
SINGLE PHASES (gram)								
Fe O (s)	0	0	0	0	0	0	0	0
Fe (s)	0	0	0	0	0	0	0	0
Fe S (s)	0	0	0	0	0	21.36	21.36	21.36

Note: The concentrations of H_2, H_2O, and CO were fixed, and CO_2 was treated as an iert gas (N_2) in the calculation.

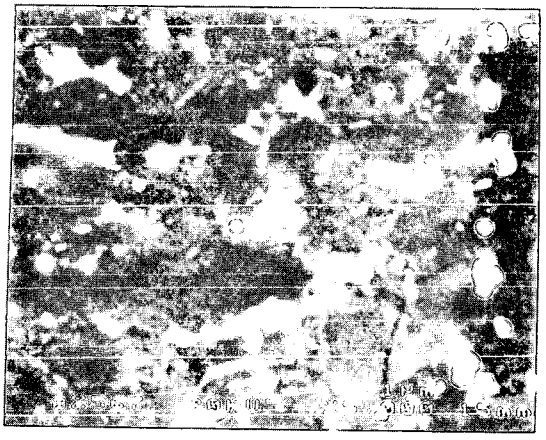

Fig. 1. SEM backscatter image of a well sintered layer in the deposit. Bright areas are iron sulfide, light grey - iron magnesium alumina silicate, and dark grey - calcium alumina silicate.

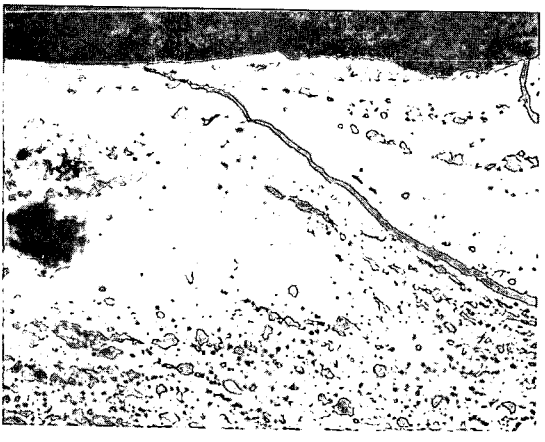

Fig. 2. Backscatter SEM image showing iron sulfide layering (bright) within a moderately sintered area of the deposit.

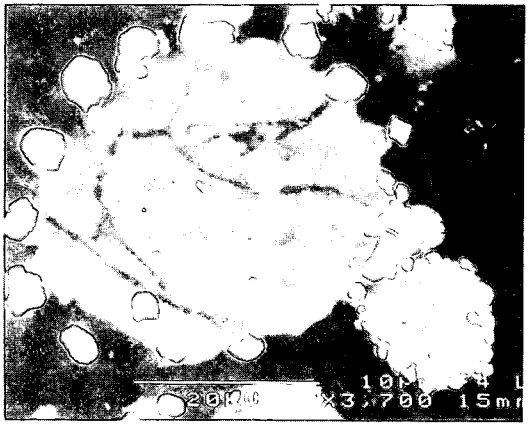

Fig. 3. Backscatter SEM image showing ash particles in a porous part of the deposit. Iron sulfide crystals (bright areas) are on the outside surface. The light grey areas are iron-magnesium alumina silicates within a calcium-potassium rich glass.

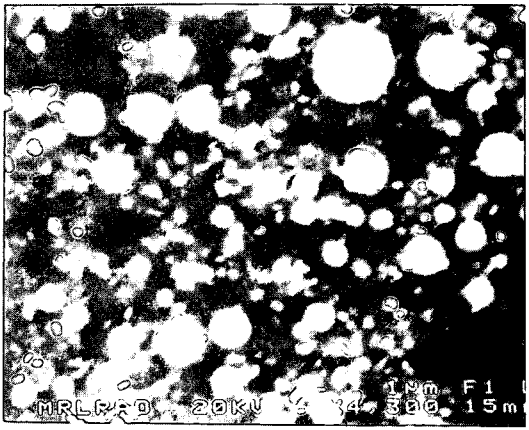

Fig. 4. SEM backscatter image of the gas exposed surface of the deposit showing an absence of sintering and devitrofication of the flyash.

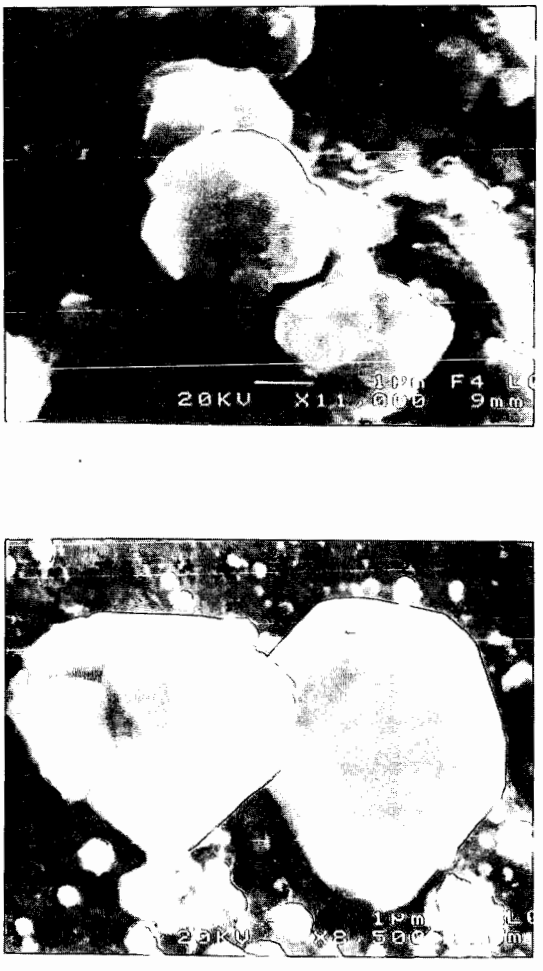

Fig. 5. SEM images of iron sulfide crystals growing on the outer surfaces of the deposit. Crystals growth can be seen occurring around siliceous particles.